

# High-fat diet feeding disrupts the coupling of thermoregulation to energy homeostasis



Jennifer D. Deem<sup>1</sup>, David Tingley<sup>2</sup>, Christina A. Watts<sup>1</sup>, Kayoko Ogimoto<sup>1</sup>, Caeley L. Bryan<sup>1</sup>, Bao Anh N. Phan<sup>1</sup>, Vincent Damian<sup>1</sup>, Michael R. Bruchas<sup>3,4,5</sup>, Jarrad M. Scarlett<sup>1,6</sup>, Michael W. Schwartz<sup>1</sup>, Gregory J. Morton<sup>1,\*</sup>

## ABSTRACT

**Objective:** Preserving core body temperature across a wide range of ambient temperatures requires adaptive changes of thermogenesis that must be offset by corresponding changes of energy intake if body fat stores are also to be preserved. Among neurons implicated in the integration of thermoregulation with energy homeostasis are those that express both neuropeptide Y (NPY) and agouti-related protein (AgRP) (referred to herein as AgRP neurons). Specifically, cold-induced activation of AgRP neurons was recently shown to be required for cold exposure to increase food intake in mice. Here, we investigated how consuming a high-fat diet (HFD) impacts various adaptive responses to cold exposure as well as the responsiveness of AgRP neurons to cold.

**Methods:** To test this, we used immunohistochemistry, in vivo fiber photometry and indirect calorimetry for continuous measures of core temperature, energy expenditure, and energy intake in both chow- and HFD-fed mice housed at different ambient temperatures.

**Results:** We show that while both core temperature and the thermogenic response to cold are maintained normally in HFD-fed mice, the increase of energy intake needed to preserve body fat stores is blunted, resulting in weight loss. Using both immunohistochemistry and in vivo fiber photometry, we show that although cold-induced AgRP neuron activation is detected regardless of diet, the number of cold-responsive neurons appears to be blunted in HFD-fed mice.

**Conclusions:** We conclude that HFD-feeding disrupts the integration of systems governing thermoregulation and energy homeostasis that protect body fat mass during cold exposure.

© 2023 The Author(s). Published by Elsevier GmbH. This is an open access article under the CC BY-NC-ND license (<http://creativecommons.org/licenses/by-nc-nd/4.0/>).

**Keywords** AgRP neurons; Core temperature; Energy expenditure; Energy intake; High-fat diet; Thermoregulation

## 1. INTRODUCTION

Maintenance of stable core body temperature during cold exposure requires rapid and effective integration of systems governing energy homeostasis and thermoregulation [1,2]. Specifically, increased energy expenditure is required to maintain core body temperature, and if this response is not associated with a corresponding increase of energy intake, body fat stores will be depleted over time. While recent evidence suggests that this integration of adaptive responses is negatively impacted by diet-induced obesity (DIO) [3], the precise nature of such an effect remains uncertain. In the current work, we therefore sought to better understand how these processes are impacted in cold-exposed mice consuming an obesogenic high-fat diet (HFD). Specifically, we analyzed the time course of changes in both energy balance and body temperature of mice that were fed either

standard chow or a HFD and were transferred from housing at room temperature (22 °C) to either a warm (30 °C) or cool (14 °C) environment.

Although agouti-related protein (AgRP) neurons are best known as drivers of the homeostatic response to energy deficit, they also play a key role in the effect of cold exposure to increase food intake [1]. Located in the hypothalamic arcuate nucleus (ARC) [4], these neurons are regulated by a variety of afferent hormonal, nutritional and neuronal-related inputs that operate over different time scales [5]. In conditions associated with negative energy balance (such as fasting or dietary weight loss), for example, AgRP neurons are activated by reduced inhibitory input conveyed by sensory, humoral and so-called “gut-brain” signals. This activation in turn elicits broad-based feeding, behavioral and metabolic responses that collectively promote positive energy balance and recovery of lost body weight [5]. The

<sup>1</sup>University of Washington Medicine Diabetes Institute, Department of Medicine, Seattle, WA, USA <sup>2</sup>Beth Israel-Deaconess Medical Center, Harvard University, School of Medicine, Boston, MA, USA <sup>3</sup>Department of Anesthesiology and Pain Medicine, University of Washington, Seattle, WA, USA <sup>4</sup>Department of Pharmacology, University of Washington, Seattle, WA, USA <sup>5</sup>Center for the Neurobiology of Addiction, Pain, and Emotion, University of Washington, Seattle, WA, USA <sup>6</sup>Department of Pediatric Gastroenterology and Hepatology, Seattle Children’s Hospital, Seattle, WA, USA

\*Corresponding author. Department of Medicine, University of Washington, UW Medicine at South Lake Union, 750 Republican St, F771, Box 358062 Seattle, WA, 98109, USA. E-mail: [gjmorton@uw.edu](mailto:gjmorton@uw.edu) (G.J. Morton).

**Abbreviations:** AgRP, agouti-related protein; ARC, arcuate nucleus; CCK, cholecystokinin; DIO, diet-induced obesity; GI, gastrointestinal; HFD, high fat diet; NPY, neuropeptide Y; MCH, melanin concentrating hormone; PBS, phosphate buffered saline; POMC, proopiomelanocortin

Received September 28, 2023 • Revision received October 26, 2023 • Accepted November 2, 2023 • Available online 4 November 2023

<https://doi.org/10.1016/j.molmet.2023.101835>

vital role played by these neurons in energy homeostasis is evident in the observation that in adult mice, the effect of fasting to increase food intake requires AgRP neuron activation [6], whereas activation of these neurons stimulates feeding irrespective of nutritional status [6–8]. Unlike the slower generation and transmission of signals generated in response to changes of energy balance or fuel stores, AgRP neurons are also regulated rapidly in response to sensory cues such as the sight, smell or taste of food that anticipate feeding [9–11]. Termed ‘allostasis’, this type of control mechanism involves the integration of internal state variables with learned experience to predict future need, rather than responding in a compensatory manner to events that have already occurred — such as a reduction in body fat stores. Among these sensory inputs is ambient temperature, as cold exposure was recently shown to rapidly activate AgRP neurons, a response that is in turn required for cold-induced hyperphagia [1].

In addition to the physiological role played by AgRP neurons, excessive or aberrant activation of these neurons is strongly implicated in the pathogenesis of obesity, diabetes and related metabolic disorders [12,13]. Thus, a critical question is whether HFD-feeding is associated with aberrant regulation of AgRP neurons. Consistent with this notion, published data reveals that in mice, consuming an obesogenic HFD attenuates the AgRP neuronal response to food presentation [14,15], to the gastro-intestinal (GI) hormones ghrelin and cholecystokinin (CCK), and to intragastric infusion of fat [14]. Combined with evidence that HFD consumption blunts the feeding response elicited by experimental AgRP neuron activation [14], these findings suggested to us that HFD feeding might also impair the normal adaptive response mounted by these neurons to promote energy homeostasis during cold exposure.

## 2. METHODS

### 2.1. Animals

All procedures were approved by the Institutional Animal Care and Use Committee at the University of Washington and performed in accordance with NIH Guide for the Care and Use of Laboratory Animals. Adult male C57/Bl6 wild-type (WT) mice were obtained from Jackson Laboratories, ME, *AgRP-IRES-Cre* mice (kindly provided to us by Dr. Streamson Chua, Jr (Albert Einstein College of Medicine)), are readily available from Jackson Laboratories and have been previously described [16] and *AgRP-Cre:GFP* knock-in mice were kindly provided by Dr. Richard Palmiter (University of Washington) and been previously described [1]. Mice were individually housed in a temperature-controlled room with either a 12:12 h or 14:10 h light:dark cycle under specific-pathogen free conditions and were provided with ad libitum access to water and fed either standard laboratory chow (5001; 13 % kcal fat, LabDiet, St. Louis, MO) or a 60 % kcal HFD (D12492; Research Diets Inc., NJ), unless otherwise stated.

### 2.2. Viral constructs

For *in vivo* fiber photometry studies, we utilized an AAV containing a Cre-dependent cassette for the genetically encoded calcium indicator, GCaMP6s, AAVDJ-EF1a-DIO-GCaMP6s-WPRE (UNC Viral Core, Chapel Hill, NC) or eYFP fluorophore control (AAV-Ef1a-DIO-eYFP-WPRE-pA, UNC Viral Core, Chapel Hill, NC).

### 2.3. Stereotaxic surgery

For stereotaxic viral injections, mice were placed in a stereotaxic frame (Kopf 1900, Cartesian Research Inc, CA) under isoflurane anesthesia. The skull was exposed with a small incision, and two small holes were drilled for unilateral microinjection (400 nl) of an AAV into the ARC of *AgRP-IRES-Cre* mice at stereotaxic coordinates based on the Mouse

Brain Atlas [17] using an angled approach: Anterior/Posterior: 1.85 mm, Dorsal/Ventral: 6.2 mm, ~12.5° angle from midline) as previously described [1,18]. Following viral injections, a fiber-optic ferrule (0.48 NA, Ø400 mm core; Doric Lenses, Quebec, Canada) was implanted using the same coordinates. All microinjections were performed using a Hamilton syringe with a 33-gauge needle at a flow rate of 100 nl/min (Micro4 controller, World Precision Instruments, FL), followed by a 5 min pause and slow withdrawal. Animals received a perioperative subcutaneous injection of buprenorphine hydrochloride (0.05 mg/kg; Reckitt Benckiser, VA). After surgery, mice were allowed 3 weeks to recover to maximize virally transduced gene expression and to acclimate animals to handling and experimental paradigms prior to study. Viral expression was verified post hoc in all animals, and any data from animals in which the virus was expressed outside the targeted area were excluded from the analysis.

### 2.4. Body composition analysis

Body composition analysis of body fat mass and lean mass was determined using quantitative magnetic resonance spectroscopy (EchoMRI 3-in-1; Echo MRI, TX) in live conscious mice with support from the NIDDK-funded Nutrition Obesity Research Center (NORC) Energy Balance Core at the University of Washington [19].

### 2.5. Indirect calorimetry

For indirect calorimetry studies, C57/Bl6 mice were acclimated to metabolic cages after which energy expenditure was measured using a computer-controlled indirect calorimetry system (Promethion®, Sable Systems, NV) with support from the NORC Energy Balance Core as described previously [1,20,21]. For each animal, O<sub>2</sub> consumption and CO<sub>2</sub> production were measured for 1-min at 5-min (acute studies) or 10-min (chronic studies) intervals. Respiratory quotient was calculated as the ratio of CO<sub>2</sub> production to O<sub>2</sub> consumption. Energy expenditure was calculated using the Weir equation [22]. Ambulatory activity was measured continuously, with consecutive adjacent infrared beam breaks in the x-, y- and z-axes scored as an activity count that was recorded every 5 or 10 min. Data acquisition and instrument control were coordinated by MetaScreen v.1.6.2 and raw data was processed using ExpeData v.1.4.3 (Sable Systems) using an analysis script documenting all aspects of data transformation.

### 2.6. Core body temperature monitoring

Adult male C57/Bl6 mice received body temperature transponders implanted into the peritoneal cavity (Starr Life Science Corp, PA) and were allowed a one-week recovery period. Animals were then acclimated to metabolic cages enclosed in temperature- and humidity-controlled cabinets (Caron Products and Services, Marietta, OH) prior to study. Signals emitted by body temperature transponders were sensed by a platform receiver positioned underneath the cage and analyzed using VitalView software as previously described [21,23].

### 2.7. Thermal challenges

To determine the effect of HFD-feeding on cold-induced Fos in AgRP neurons, 12-wk HFD-fed *AgRP-Cre:GFP* mice were housed in temperature-controlled chambers pre-set overnight at either 22 °C, 30 °C, or 14 °C for 90 min without access to food. To examine the effect of chronic mild-cold exposure on comprehensive measures of energy homeostasis in the setting of HFD-feeding, both chow- and 12 wk HFD-fed mice were acclimated to metabolic cages housed within temperature- and humidity-controlled chambers, and either remained at 22.0 ± 0.1 °C or were exposed to 14.0 ± 0.1 °C or 30.0 ± 0.1 °C for 5 days. During this period, continuous measures of

energy expenditure, respiratory quotient, ambulatory activity, body temperature and energy and water intake were recorded, and body composition was determined both before and after the thermogenic challenge. To examine the time-course effect of HFD feeding on the acute feeding and thermogenic response to cold exposure, we first conducted baseline recordings in WT chow-fed mice in which animals were rapidly transferred to metabolic cages housed within temperature-controlled chambers preset to either 14 °C or 22 °C and studied for 4 h. Animals were then placed on a HFD for the duration of the experiment and were studied after 1, 2, 5, 8, 10 and 12 wk after HFD-feeding.

### 2.8. In vivo fiber photometry

For in vivo fiber photometry recordings of AgRP neurons in response to cold exposure, mice were acutely housed on a custom thermal platform. Baseline GCaMP6s fluorescence signals were set to similar levels across animals by adjusting the intensities of the 470 nm and 405 nm LEDs, and a baseline recording was measured for 5 min. For temperature-challenge studies, mice were placed in a small custom-built plexiglass temperature chamber (3' × 6' × 6') that was constructed to enclose a Peltier cooler platform that could be controlled by an external controller (TE Tech, TC720) as described [1,24]. Animals were acclimated on three separate days to tether and Peltier platform. For temperature ramp studies, animals were attached to tether and allowed 2–3 min for photobleaching before photometry recording is initiated. Temperature-ramp studies were designed to test GCaMP6s activity in AgRP neurons when transitioning from 30 °C to 10 °C or 10 °C to 30 °C. Animals were held at 30 °C for 10 min before transitioning to 10 °C for 10 min before returning to 30 °C with each temperature ramp repeated twice during a recording session. Transitions between temperatures were all set to 60 s. Experiments were aligned initially to 22 °C. As an added positive control, at the end of each study, animals were presented with a food pellet, which led to an expected reduction in AgRP neuron activity [9,10]. Prior to study, chow-fed mice were acclimated to experimental procedures and AgRP-calcium responses to food presentation in a fast-refeed paradigm was used as a positive control to indicate successfully targeted animals. Briefly, overnight-fasted animals that failed to demonstrate ≥10 % reduction in  $\Delta F/F$  in response to chow presentation were identified as surgical misses and excluded from further study. Following these baseline recordings, animals that passed the inclusion criteria either remained on chow, or were placed on a HFD and studied again 1, 2, 5, 8 and 10 wk later. Accurate viral targeting and fiber-optic placement were verified post hoc in all animals, and data from improperly targeted animals were excluded from the analysis.

### 2.9. Immunohistochemistry

For immunohistochemical studies, animals were overdosed with ketamine:xylazine and perfused with 1× phosphate-buffered saline (PBS) followed by 4 % (v/v) paraformaldehyde in 0.1 M PBS. Brains were removed and post-fixed for 4 h in paraformaldehyde followed by sucrose (30 %) dehydration and embedded in optimal cutting temperature compound blocks. Free-floating coronal sections were obtained via Cryostat at 35 μm thickness and stored in 1× PBS with 0.02 % sodium azide at 4 °C. Free-floating sections were then washed at room temperature in phosphate-buffered saline with Tween 20 (PBS-T) for 1 h, followed by a blocking buffer (5 % normal donkey serum, 1 % bovine serum albumin in 0.1 M PBS-T with azide) for an additional hour with rocking. Sections were then incubated 24–48 h at 4 °C with polyclonal rabbit anti-cFos (Millipore, Ab-5 4–17, 1:10,000; RRID: AB\_2106755) and/or Chicken anti-GFP (Abcam, ab13970,

1:10,000; RRID: AB\_300798) in blocking buffer. Following a set of washes in PBS-T at room temperature, sections were incubated in secondary donkey anti-rabbit Alexa 594 or donkey anti-chicken Alexa 488 (1:500; Jackson ImmunoResearch Laboratories, PA) diluted overnight at 4 °C, followed by a final set of washes in PBS-T. To provide a nuclear contrast stain, sections were incubated with DAPI (Sigma–Aldrich, MBD0015, 1:1000) in PBS for 10 min at room temperature, followed by 5 additional washes in PBS-T. Sections were then mounted with Fluoromount-G with DAPI (ThermoFisher, 00-4959-52) or polyvinyl acetate.

### 2.10. Quantification of Fos + cells

Immunostaining for Fos was quantified by imaging at either 10× or 20× on a Leica SP8X confocal system with support from the University of Washington, W.M. Keck Microscopy Center. Images were merged using ImageJ (Fiji, NIH) and threshold adjusted to minimize nonspecific background fluorescence. Fos + cells were then identified and counted in 35 μm sections obtained serially across the full rostral to caudal axis of the arcuate nucleus using the 'analyze particles' feature, such that consistent fluorescence and size thresholds were used throughout, as previously described [1,25].

### 2.11. qRT-PCR

To measure hypothalamic transcripts, at study completion, mice were sacrificed and the hypothalamus was rapidly dissected and flash frozen. Individual tissue samples were dounce homogenized and RNA was isolated using Qiagen RNeasy Micro Kit (Kit# 74004, Hilden, Germany) and isolated RNA concentrations were quantified by Nanodrop (Thermo Fisher Scientific, DE). qRT-PCR was performed using SYBR Green One-Step (Kit# 600825, Agilent, CA). qRT-PCR data were analyzed using the Sequence Detection System software (SDS Version 2.2; Applied Biosystems, CA). Expression levels of each gene were normalized to a housekeeping gene (18S RNA) and standard curve. Non-template controls were incorporated into each PCR run. Oligonucleotides selected were Agouti-related protein (*Agrp*): For: 5'-ATG CTG ACT CGA ATG TTG CTG-3', Rev: 5'-CAG ACT TAG ACC TGG GAA CTC T-3', Pro-opiomelanocortin (*Pomc*): For: 5'-CAG TGC CAG GAC CTC AC-3', Rev: 5'-CAG CGA GAG GTC GAG TTT G-3', Neuropeptide Y (*Npy*): For: 5'-CTC CGC TCT GCG ACA CTA C-3', Rev: 5'-AGG GTC TTC AAG CCT TGT TCT-3', Pro-melanin concentrating hormone (*Mch*): For: 5'-GAA TTT GGA AGA TGA CAT AGT AT-3', Rev: 5'-CCT GAG CAT GTC AAA ATC TCT CC-3', 18S Ribosomal RNA (*18S*): For: 5'-CGG ACA GGA TTG ACA GAT TG-3', Rev: 5'-CAA ATC GCT CCA CCA ACT AA-3'.

### 2.12. Statistical analyses

Results are expressed as mean ± SEM. Significance was established at  $p < 0.05$ , two-tailed. For statistical comparisons involving measures of core temperature, energy expenditure, ambulatory activity, respiratory quotient or energy intake over multiple days, data obtained during the 14 °C and 22 °C test periods were reduced into average light and dark photoperiods and 24 h means for each mouse. A group by ambient temperature ANOVA with least significance difference pairwise tests compared mean values between groups. Where applicable, time-series data were analyzed using treatment by time-mixed factorial ANOVA or linear-mixed model analysis controlling for within-subjects correlated data using a random intercept model with treatment and time as fixed effects [26]. A two-sample unpaired Student's *t*-test was used for two-group comparisons, a paired *t*-test for within group comparisons, a one-way ANOVA to compare mean values among multiple groups and for Fos studies, data was analyzed using a two-way ANOVA (diet × ambient temperature). All post hoc comparisons were

determined using Sidak correction for multiple comparisons. Statistical analyses were performed using SPSS (SPSS version 23, IBM Corp., Somers, NY), R (version 3.6.2; R Project for Statistical Computing, RRID: SCR\_001905), python, MATLAB (MathWorks; MA) and GraphPad Prism (version 7.4; CA; RRID: SCR\_002798).

### 3. RESULTS

#### 3.1. Effect of DIO on determinants of energy homeostasis in mice chronically exposed to different thermal environments

To determine the impact of DIO on the coupling of thermoregulation to energy homeostasis, we measured the effect of mild cold exposure (14 °C) in comparison to housing at either 22 °C or 30 °C on food intake, energy expenditure and body temperature over a 5-day period. These studies were performed in adult male WT mice maintained on either standard chow or on a HFD for 12 weeks, a duration sufficient to

cause DIO (mean body weight: 30.68 ± 0.31 g for chow vs. 44.88 ± 0.87 g for HFD;  $p < 0.05$ ). Consistent with the previous studies [2,21,27,28], WT chow-fed mice maintained their core body temperature within the normal range across each of three ambient temperatures. These animals also exhibited the expected diurnal rhythm of body temperature irrespective of ambient temperature (Figure 1A). While core body temperature also remained stable across thermal environments in mice fed a HFD, the temperature that they maintained was slightly elevated relative to chow-fed controls, as previously reported [29] (Figure 1B and C). Both the expected increase of energy expenditure when housed at 14 °C and the compensatory reduction of energy expenditure when housed at 30 °C were also observed in both chow- and HFD-fed mice (Figure 1D–F). Thus, the inverse relationship between energy expenditure and ambient temperature characteristic of normal animals was preserved in DIO mice [3,21,30] (Figure 1J).

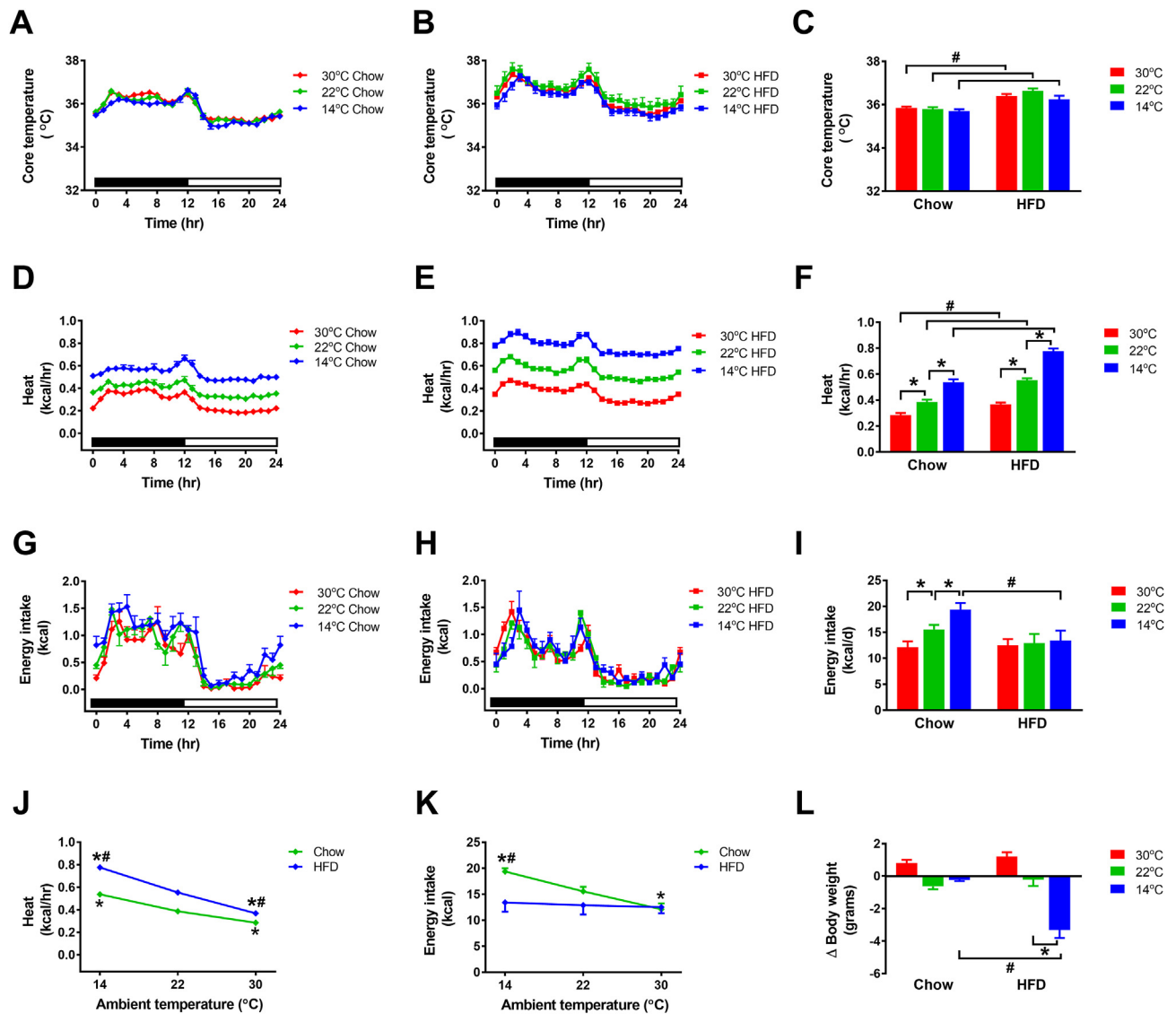


**Figure 1: Effect of ambient temperature on energy homeostasis in DIO mice.** Photoperiod-averaged 24-h profiles and mean measures of (A–C) core temperature, (D–F) heat production and (G–I) energy intake, the relationship between (J) heat production and (K) energy intake and ambient temperature, and (L) change in body weight in adult male wild-type mice fed either standard laboratory chow or high-fat diet for 12 weeks that were housed at either 14 °C, 22 °C and 30 °C for five days.  $n = 8$  per group. Mean ± SEM. \* $p < 0.05$  vs. 22 °C, # $p < 0.05$  vs. chow.

Previous work has shown that in chow-fed mice, the increase of energy expenditure associated with sub-thermoneutral housing was also accompanied by an increase of respiratory quotient, suggestive of an increased rate of carbohydrate oxidation [21]. In animals consuming a HFD, however, respiratory quotient remained lower than in mice consuming chow (indicative of increased fatty acid oxidation), irrespective of ambient temperature, presumably driven by their higher dietary fat content (Supplementary Figure 1A–C). The increase of energy expenditure during mild cold exposure was not attributable to differences in ambulatory activity levels in either group, as these remained similar across different ambient temperatures (Supplementary Figure 1D–F), consistent with the previous findings [21,23]. In normal mice maintained on a standard chow diet, the effect of cold exposure to increase energy expenditure is matched by a proportionate increase of energy uptake, resulting in a strong inverse correlation between energy intake and ambient temperature [21,30], and our findings in chow-fed control mice confirm this relationship (Figure 1K). Specifically, consistent with the previous findings [3,21,30,31], we found that relative to housing at 22 °C, energy intake declined when the animals were housed at 30 °C, and was increased at 14 °C (Figure 1G and I). Moreover, these compensatory adjustments of energy intake in chow-fed mice precisely offset the energy demands associated with each thermal environment such that neither body weight nor body fat mass changed despite marked differences in the amount of energy consumed (Figure 1L). These findings highlight the well-documented integration of systems governing energy homeostasis and thermoregulation, such that neither body temperature nor body weight change despite marked changes of fuel flux mounted in response to housing in different ambient temperatures [2,32]. It is in this context that differences between chow- and HFD-fed mice are notable.

First, total energy expenditure (measured on a per animal basis) was greater in DIO mice than chow-fed controls irrespective of ambient temperature, as expected given their larger body mass. More importantly, the inverse relationship between food intake and ambient temperature was absent in mice rendered obese by HFD feeding for

12 wk (Figure 1K). Relative to energy intake at 22 °C, DIO mice did not reduce their intake when housed at 30 °C, nor did they increase the energy intake in response to mild cold exposure (14 °C) (Figure 1H and I). Stated differently, the normal coupling of energy homeostasis to thermoregulation is disrupted in mice with DIO, and because energy intake remained constant irrespective of ambient temperature (Figure 1K), these animals exhibited significant weight loss when housed at 14 °C, consistent with previous observations [3] (Figure 1L).

### 3.2. Effect of acute mild cold exposure on energy expenditure and energy intake in DIO mice

Our previous findings show that in normal mice fed a standard chow diet, both energy expenditure and energy intake are rapidly increased in response to cold exposure [1]. Here, we examined the effects on food intake and energy expenditure of rapidly transferring mice with DIO (induced by consuming a HFD for 12-wk), from housing at 22 °C to 14 °C. Consistent with our findings using the chronic housing paradigm, energy expenditure increased rapidly following the transfer from 22 °C to 14 °C in HFD-fed mice, and it remained elevated for the duration of the study (Figure 2A–D). However, in contrast to our previous findings in chow-fed mice [1], food intake failed to increase in response to acute cold exposure in HFD-fed mice (Figure 2E–H). We interpret this failure to mount the hyperphagic response needed to defend body weight in the face of a thermal challenge as a defect in the central mechanisms that couple energy homeostasis and thermoregulation to one another.

### 3.3. Effect of short-term HFD-feeding on the adaptive response to cold exposure

A key question raised by these findings is whether the establishment of DIO is required for the effect of a HFD to block compensatory hyperphagia and prevent weight loss during cold exposure. To address this question, we studied mice that had been placed on a HFD but had yet to experience significant weight gain relative to chow-fed controls (Figure 3A). Specifically, after being placed on a HFD for 12 d or remaining on chow, mice were placed in temperature- and humidity-

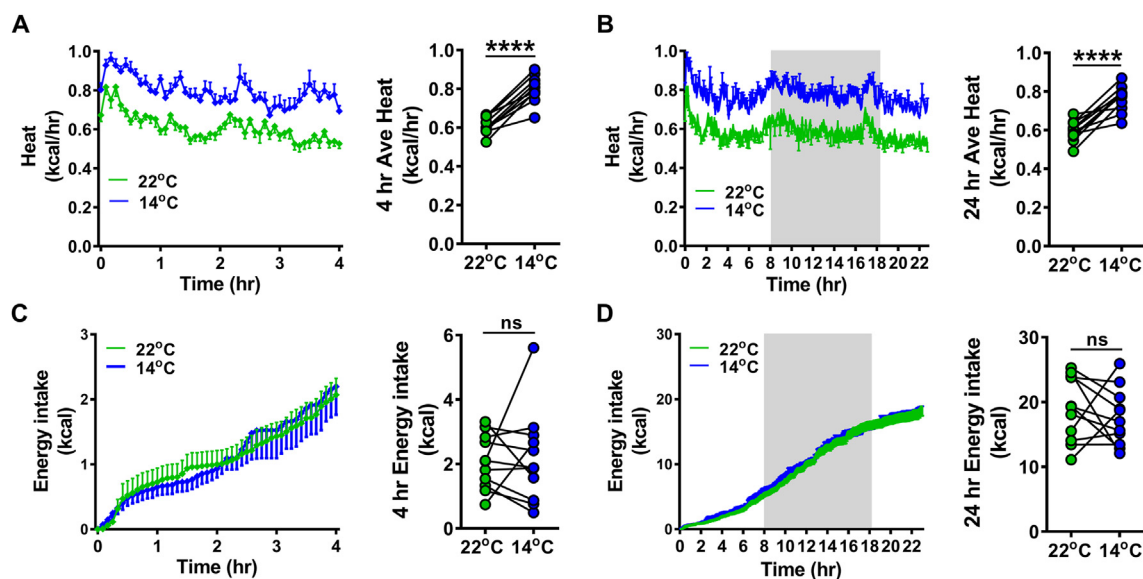


**Figure 2: Effect of acute mild cold exposure to rapidly increase energy intake is blunted in DIO mice.** Time-course and mean (A and B) heat production and (C and D) energy intake measured over (A and C) 4 h or (B and D) 24 h in adult male wild-type mice fed either standard laboratory chow or high-fat fed for 12 weeks and acutely housed at either 14 °C or 22 °C.  $n = 11$  per group. Mean  $\pm$  SEM. \*\*\*\* $p < 0.0001$ .

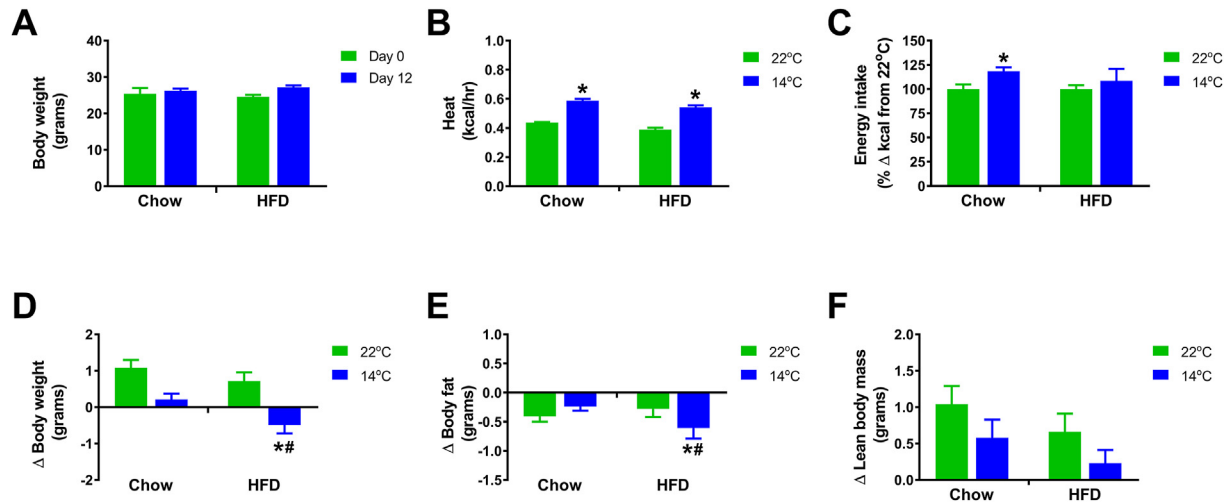


**Figure 3: Effect of short-term HFD feeding on the adaptive response to cold exposure** (A) Body weight in adult male wild-type mice at the onset and 12 days following exposure to standard laboratory chow or high-fat diet. (B) Mean heat production, (C) percent change in energy intake, (D) change in body weight, (E) change in body fat and (F) change in lean body mass in adult male wild-type mice fed either standard laboratory chow or high-fat fed for 12 days that were then studied for five consecutive days using indirect calorimetry at 22 °C, followed by an additional five consecutive days at 14 °C.  $n = 8$  per group. Mean  $\pm$  SEM. \* $p < 0.05$  vs. 22 °C, # $p < 0.05$  vs. chow.

controlled indirect calorimetry chambers set at 22 °C for 5 days before being subjected to mild cold exposure (14 °C) for an additional 5 days. Similar to our earlier observations, both chow and HFD-fed mice increased their energy expenditure during mild cold exposure (Figure 3B). Unlike chow-fed controls, however, HFD-fed mice failed to increase their energy intake (Figure 3C). Consequently, whereas the body weight of chow-fed animals was not impacted by mild cold exposure, body weight decreased significantly in HFD-fed mice, an effect associated with a significant loss in body fat stores (Figure 3D and E). Thus, the impaired hyperphagic response to cold exposure is detectable in HFD-fed mice prior to the establishment of DIO.

### 3.4. Time-course effect of HFD-feeding on cold-induced hyperphagia

We next determined the time-course over which switching from standard chow to a HFD blunts the adaptive feeding response to cold exposure. Consistent with data presented above and with the previous reports [1,33], we found that at baseline (prior to the diet switch), both energy intake and energy expenditure increased rapidly in response to cold exposure (Figure 4A and B). Following the switch to a HFD, the cold-induced increase of energy expenditure remained intact (Figure 4). In contrast, however, cold-induced hyperphagia was blunted within 1 wk of the onset of HFD feeding, and this blunting persisted throughout the study (Figure 4). Thus, HFD-feeding disrupts cold-induced hyperphagia in a matter of days, prior to the onset of DIO.

### 3.5. Effect of DIO on the AgRP neuron response to chronic mild cold exposure

Based on published evidence that AgRP neurons are rapidly activated by cold exposure [1] and that HFD feeding disrupts normal regulation of AgRP neuron activity [14,15], we next sought to determine whether DIO impacts the response of AgRP neurons to a cold challenge. As a first step, we investigated the impact of a 5-day period of either mild cold exposure (14 °C) or housing at room temperature (22 °C) on hypothalamic *AgRP* mRNA levels. Prior to study, mice were maintained on either chow or fed a HFD for 12 weeks to cause DIO. To control for

differences of energy intake between groups during the period of cold exposure (when food intake increases in chow-fed but not HFD-fed mice), chow-fed animals were pair-fed to the comparatively lower energy intake of mice consuming the HFD (on a per calorie basis). As predicted, consistent with our recent observations in ad libitum chow-fed mice [1], *AgRP* and *Npy* mRNA levels increased significantly in chow-fed mice housed at 14 °C relative to 22 °C (Figure 5A), whereas DIO mice failed to mount the expected increase of hypothalamic *AgRP* gene expression (Figure 5B).

### 3.6. Effect of DIO on cold-induced activation of Fos in AgRP neurons

To investigate the effect of DIO on AgRP neuron responsiveness in a different way, we utilized transgenic AgRP-Cre:GFP mice to enable visualization of the induction of Fos protein, a marker of neuronal activation, selectively in AgRP neurons. We transferred age-matched, chow-fed controls and mice with DIO induced by consuming a HFD for 12 wk, into cages previous set to either 14 °C, 22 °C, or 30 °C for 90-min. Consistent with our previous findings [1], we found that in chow-fed controls, the percent of AgRP neurons expressing c-Fos was increased in mice housed at 14 °C relative to either 22 °C or 30 °C (Figure 6C–E). While cold exposure also increased the % of Fos + AgRP neurons in HFD-fed mice, the baseline level of Fos + AgRP neurons was reduced compared to chow-fed controls (Figure 6C–E). These findings suggest that 1) AgRP neurons are activated in response to cold in mice consuming a HFD, but that 2) the baseline level of AgRP neuron activation was comparatively low in these mice.

From these observations, we infer that the overall number of AgRP neurons activated during cold exposure is lower in mice with DIO than in chow-fed mice. It is worth mentioning that in normal, chow-fed mice, the % of AgRP neurons activated by cold exposure based on c-Fos staining (~20 %) is low in comparison to other provocative stimuli such as fasting or ghrelin administration (~70–80 %) [34,35]. We interpret this discrepancy as evidence that cold exposure activates only a small subset of all AgRP neurons, and in light of our current data, the subset that can be activated by cold appears to be further reduced in DIO mice.

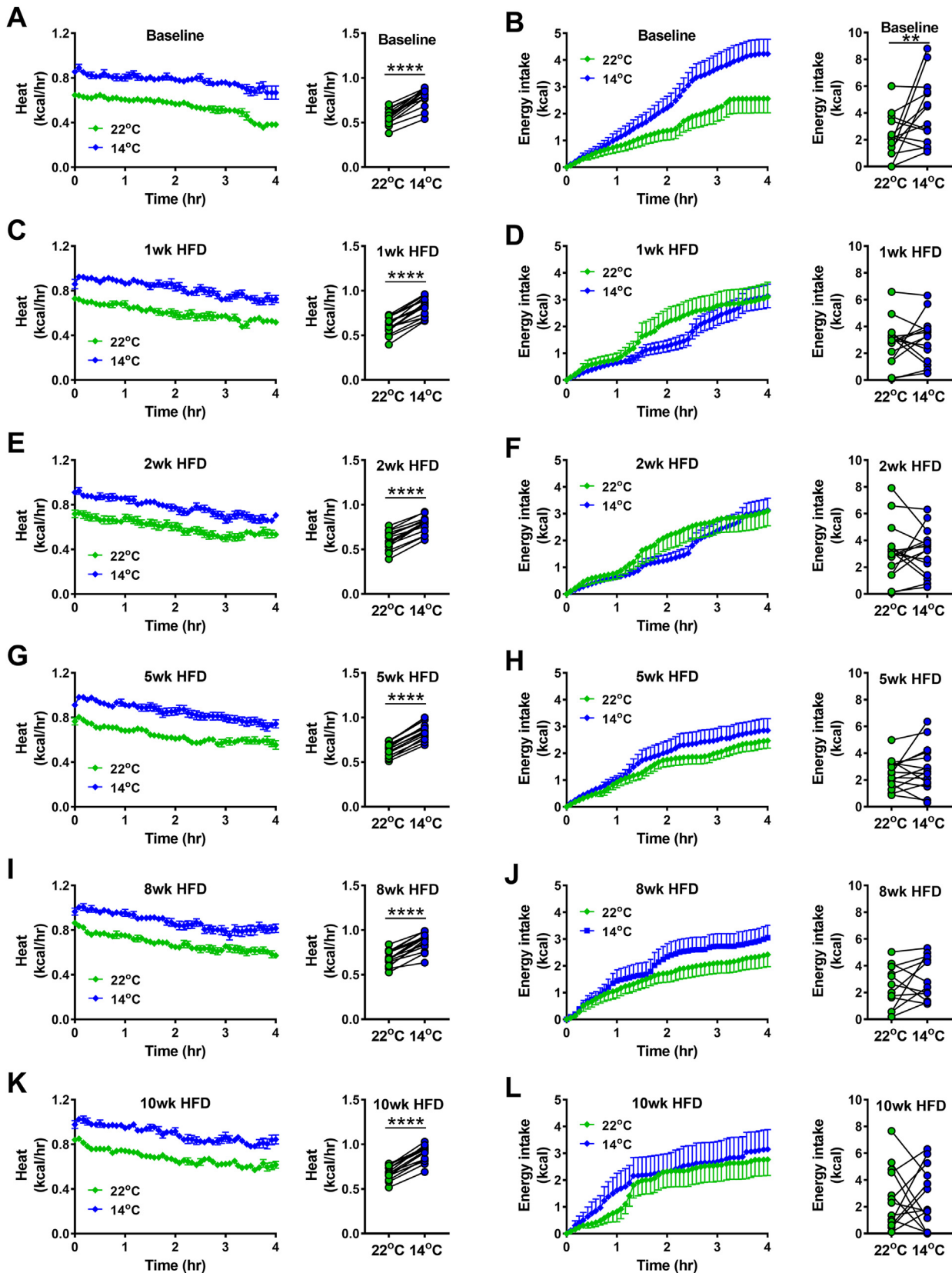


**Figure 4: Time-course effect of HFD feeding on cold-induced thermogenesis and hyperphagia.** Time-course and mean (A, C, E, G, I and K) heat production and (B, D, F, H, J and L) energy intake following exposure to either 14 °C or 22 °C for 4 h at baseline in (A and B) chow-fed mice and (C and D) 1 wk, (E and F) 2 wk, (G and H) 5 wk, (I and J) 8 wk and (K and L) 10 wk following exposure to a high-fat diet.  $n = 10\text{--}16$  per group. Mean  $\pm$  SEM. \*\*\*\* $p < 0.0001$ , \*\* $p < 0.01$ .

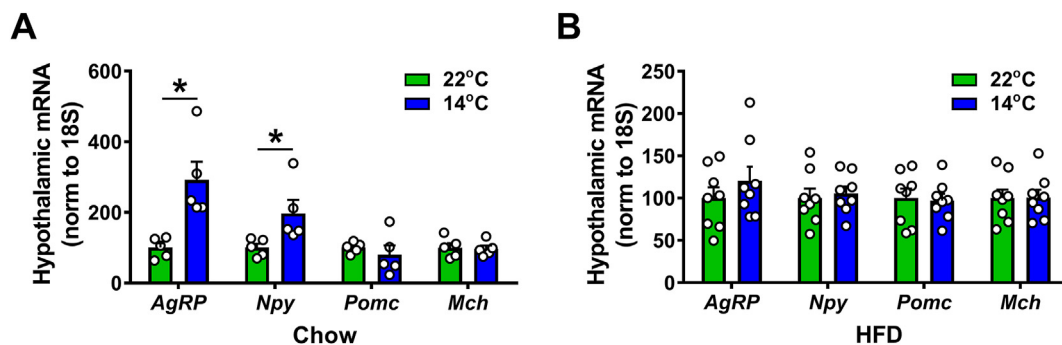


**Figure 5: Effect of DIO on *AgRP* mRNA levels in response to chronic cold exposure.** Hypothalamic mRNA levels of agouti-related protein (*AgRP*), Neuropeptide Y (*Npy*), pro-opiomelanocortin (*Pomc*) and melanin concentrating hormone (*Mch*) in adult male wild-type mice maintained on either (A) standard chow or (B) high-fat diet for 12 wk and exposed to either 22 °C or 14 °C for 5 days. To control for differences in energy intake during cold exposure, chow-fed mice were pair-fed to the intake of high-fat diet fed mice.  $n = 8-10$  per group. Mean  $\pm$  SEM. \* $p < 0.05$  vs. 22 °C.

### 3.7. Time-course effect of HFD-feeding on cold-induced increases in *AgRP* neuronal activity

To investigate the time-course of the effect of HFD feeding on cold-induced *AgRP* neuron activation in vivo, we next used fiber photometry to make serial measurements of the effect of cold exposure on the calcium activity of *AgRP* neurons of mice fed either standard chow or the HFD. Specifically, fiber photometry data was collected prior to and at 1, 2, 5, 8, and 10 wk after either switching to the HFD or continuing to consume standard chow. Prior to study, the fiber photometry method was validated by demonstrating that in fasted mice, *AgRP* neuron activity is strongly and rapidly inhibited by food presentation [9–11]. As expected [1], the *AgRP* GCaMP signal increased in within seconds of rapidly lowering the temperature of the platform from 30 °C to 10 °C in chow-fed mice, prior to the diet switch. Interestingly, this cold-induced activation response persisted throughout the study, irrespective of diet (Figure 7).

To explain this apparent discrepancy between the effect of HFD feeding on the *AgRP* response to cold detected by *c-Fos* staining vs. in vivo fiber photometry, we note that while the latter can quantify the changes in neuronal calcium activity of a population of neurons (relative to a baseline level), the method provides no insight into 1) the number of neurons that are responsive to a particular stimulus; 2) whether the stimulus impacts baseline neuron activity; or 3) the degree of heterogeneity across different neurons. A related caveat of these findings is that the magnitude of the increase of *AgRP* neuron calcium activity we observed in response to cold exposure is modest in comparison to other interventions. As one example, the inhibitory effect of food presentation in fasted mice is greater than the increase of  $dF/F$  (%) in response to cold exposure [1,9,10].

Based on these limitations, it is apparent that the number of cold-responsive *AgRP* neurons could have differed between the diet groups, despite the fact that the *AgRP* neuron photometry response to cold exposure was not affected by consuming the HFD. Consistent with this hypothesis is our *c-Fos* data (Figure 6C–E) showing that the fraction of *AgRP* neurons activated in response to cold is lower in mice consuming the HFD than standard chow. Taken together, we interpret these data to suggest that although we are able to detect cold-induced *AgRP* neuron activation in mice consuming a HFD, the relatively small number of cold-responsive *AgRP* neurons detected in chow-fed mice is further reduced by HFD consumption. Whether this reduction underlies the lack of a cold-induced hyperphagia response in HFD-fed mice awaits further study.

## 4. DISCUSSION

The ability of mammals to maintain both core body temperature and body fat mass within narrow limits across a wide range of ambient temperatures hinges on effective coupling of thermoregulation and energy homeostasis [2,21]. During cold exposure, for example, the rapid and marked increase in energy expenditure required to prevent core temperature from falling is offset by a compensatory increase in energy intake that preserves body fat stores [21,31,36]. The current work was undertaken to determine whether this adaptive coupling process is impaired by HFD feeding.

Consistent with this hypothesis, we report that the normal coupling of energy homeostasis to thermoregulation is impaired by HFD feeding, and that this effect occurs fairly quickly (within a matter of days). Specifically, we report that whereas the inverse relationship between energy expenditure and ambient temperature characteristic of normal animals [2,3,21,30] is preserved in HFD-fed mice, and while these mice preserve core body temperature irrespective of variation in external temperature, they do not exhibit the adaptive changes of food intake exhibited by chow-fed mice when the external temperature changes. Consequently, the strong inverse association between ambient temperature and energy intake observed across all mammalian species [21,30,32,37,38] is disrupted in HFD-fed mice.

Specifically, while chow-fed mice exhibit an appropriate, compensatory reduction of energy intake in response to the reduced thermogenic demands of being housed at  $\sim$ thermoneutrality, HFD-fed mice fail to make this adjustment of energy intake and thus tend to gain weight. Consequently, HFD-fed mice can become more obese when housed in a thermoneutral environment [39–42], although this is not universally observed [43]. Similarly, mice consuming a HFD fail to exhibit the expected increase of energy intake during chronic mild cold exposure, causing them to mobilize their fat stores to support heightened thermogenic needs, and thereby lose both body weight and body fat stores [3]. Moreover, we report that this impairment is detectable within a week of HFD feeding, prior to the establishment of DIO. We therefore infer that obesity is not required for the effect. Additional study however, is required to identify the mechanism(s) whereby HFD consumption impairs the hyperphagic response induced by cold exposure, including distinguishing between exposure to HFD itself vs. metabolic consequences of HFD exposure.



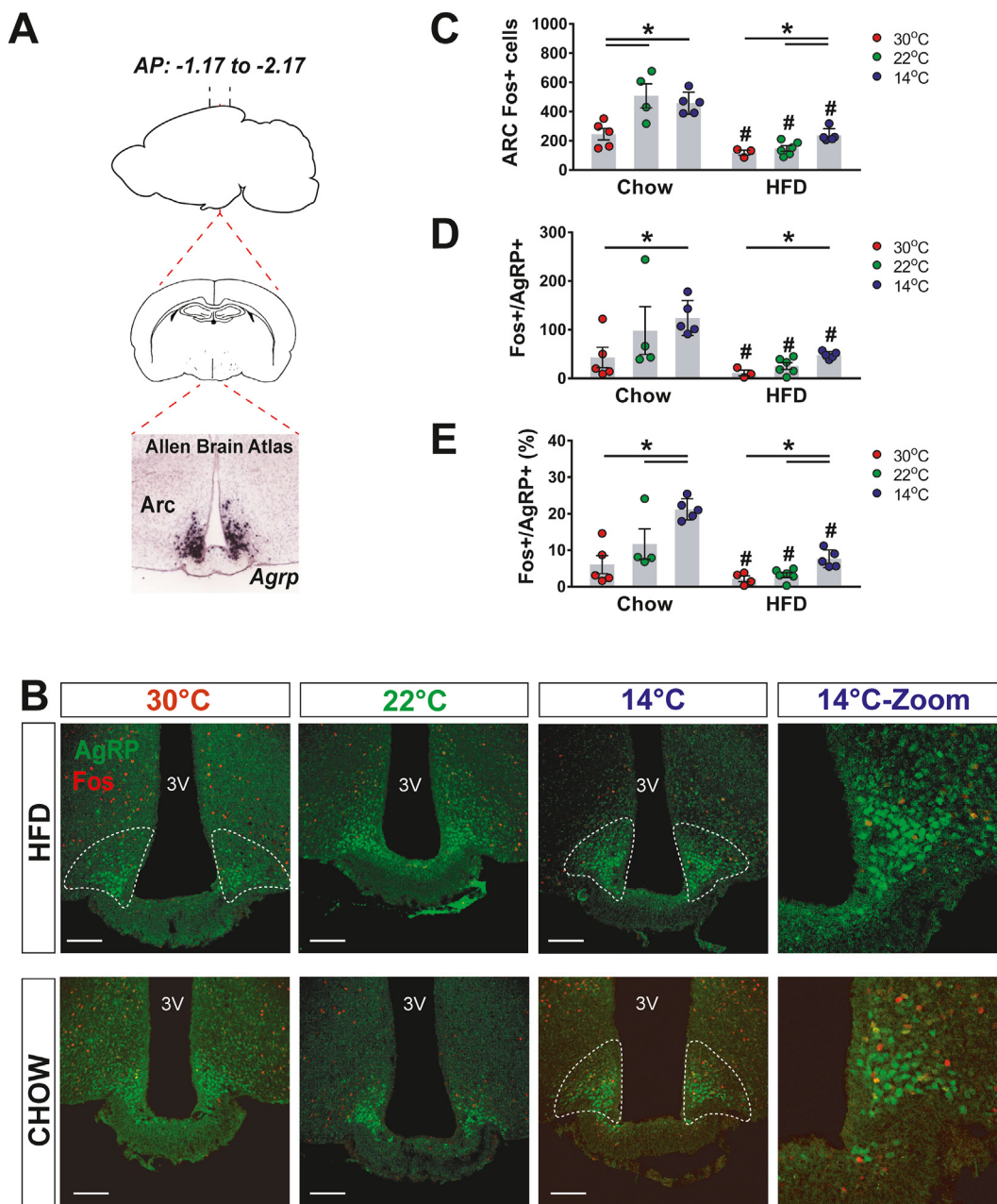


**Figure 6: Effect of DIO on cold-induced activation of Fos in AgRP neurons.** (A) Representative sagittal and coronal images and AgRP hybridization in situ from Allen Brain Institute of the arcuate nucleus (ARC). (B) Immunohistochemical detection of AgRP-locus driven green fluorescent protein (GFP) (green), Fos (red), and colocalization of GFP and Fos (two right panels) in the ARC of either chow-fed or 12-wk high-fat diet fed AgRP-Cre:GFP mice 90 min after housing at either 14 °C, 22 °C, or 30 °C. Quantitation of (C) total ARC Fos + cells, and the (D) total number and (E) percentage of AgRP neurons that co-express Fos in the ARC.  $n = 3-6$  per group. Mean  $\pm$  SEM. \* $p < 0.05$ ; # $p < 0.05$  vs. Chow.

These observations have interesting implications for the pathogenesis and treatment of obesity. On the one hand, the observation that HFD-fed mice exhibit an impaired ability to suppress energy intake at higher ambient temperatures suggests an obesogenic effect of warmer environments when this type of diet is consumed. In support of this possibility, epidemiological evidence suggests that among certain populations, ambient temperature and obesity prevalence are positively correlated [44,45]. Combined with evidence that both obesity prevalence and global temperatures have risen in recent decades, it is

tempting to speculate a causal link, and studies that test this hypothesis – and the related notion that cooler environments can reduce obesity risk among those consuming a HFD – will be of interest. We recently reported that AgRP neurons are activated within seconds of cold exposure, and the effect of cold exposure to increase energy intake, but not effect on energy expenditure, is dependent on the activation of these neurons [1]. Furthermore, the responsiveness of AgRP neurons to most known afferent inputs is blunted by consuming a HFD [14,15], and our current work shows that cold-induced

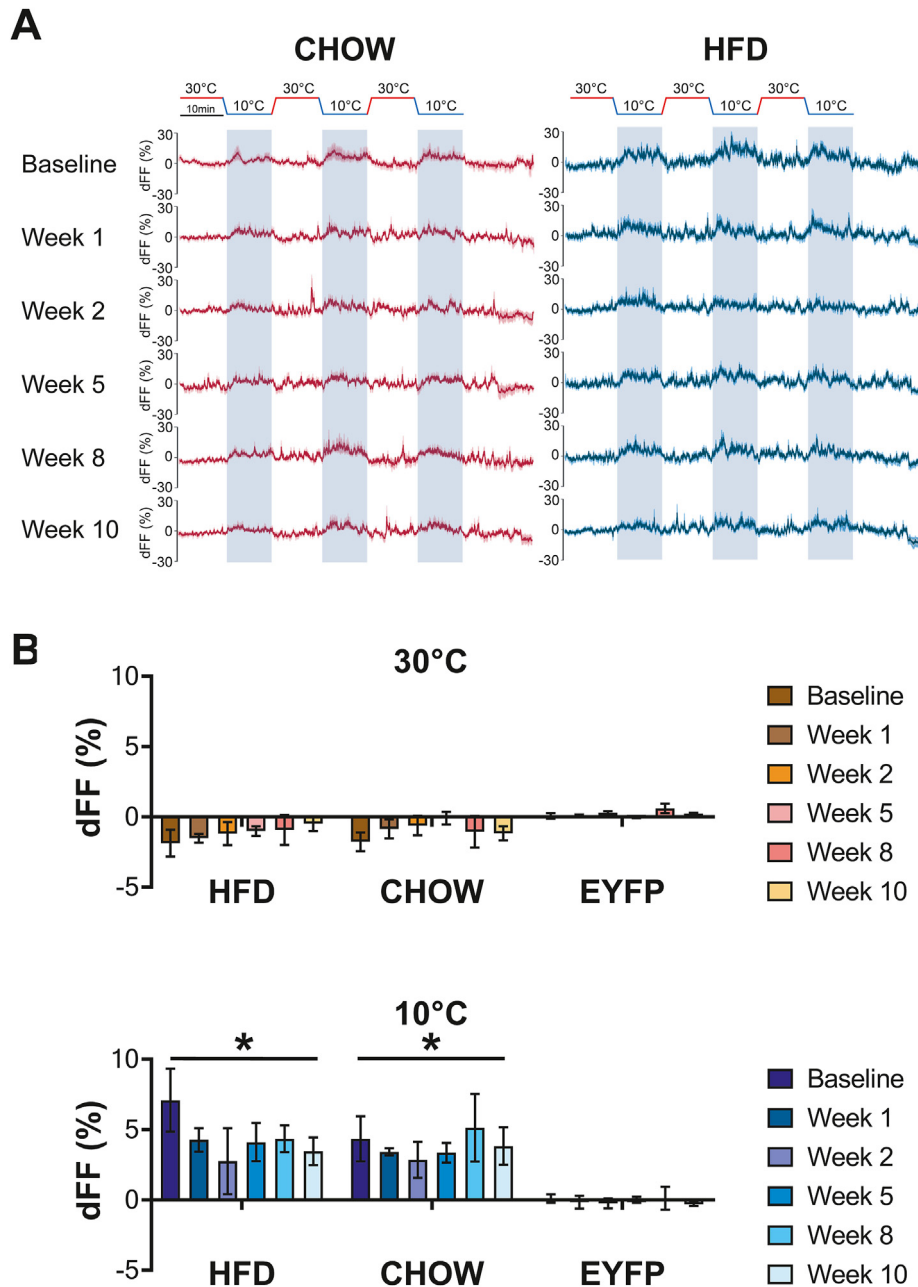


**Figure 7: Time-course effect of high-fat diet feeding on cold-induced increases in AgRP neuronal activity.** (A) Trace of averaged dF/F (%) GCaMP6s signal and (B) quantification of mean dF/F (%) differences between 30 °C and 10 °C GCaMP6s activity during 10 min exposure at baseline in chow-fed animals and at weeks 1, 2, 5, 8, and 10 in either chow-fed or high-fat diet fed mice. Transition ramps between temperatures were all set to 60 s. Gray bar signifies 10-min at 10 °C.  $n = 6$  per group. Mean  $\pm$  SEM. \* $p < 0.05$  vs. EYFP.

hyperphagia is also blunted by consuming a HFD. We therefore sought to test the hypothesis that cold-induced activation of AgRP neurons is blunted by this diet.

Consistent with the previous findings [1,33], we show that cold exposure rapidly activates AgRP neurons, and that the activity of these neurons is lower at 30 °C (~thermoneutrality) than either 22 °C or 14 °C. Moreover, whereas a majority of AgRP neurons is activated by the interventions such as fasting [35] and ghrelin administration [34], only a small fraction (~20 %) is activated by cold. Together, these observations suggest the existence of functionally distinct subsets of AgRP neurons [46], and that the subset activated by cold exposure

drives feeding, but not most other responses elicited by global AgRP activation, such as reduced thermogenesis or insulin resistance [13]. Although the interpretation of our AgRP neuron data is not entirely straightforward, our findings are consistent with a role for reduced AgRP neuron activity in the effect of a HFD to impair cold-induced hyperphagia.

This interpretation is based in part on our c-Fos data showing that in high-fat, DIO mice, 1) the baseline level of AgRP neuron activity (i.e., number of active neurons) is reduced compared to chow-fed mice, and 2) the small percentage of AgRP neurons that are responsive to cold in chow-fed controls, is smaller still in the HFD-fed group. In this context,

we note that while fiber photometry can assess the response of a population of neurons to changes of afferent input, it cannot detect either group differences of baseline activity or changes of activity in the same animal that might develop over longer periods of time (days or weeks). Thus, even though a subset of AgRP neurons remains responsive to cold (based on both fiber photometry and c-Fos staining), our data suggest that the overall number of active neurons is reduced by consuming a HFD. Additional studies are warranted to determine whether this decrease of AgRP neuron activity contributes to the effect of a HFD to blunt the cold-induced hyperphagic response.

This outcome closely resembles the effect of HFD-feeding to blunt the AgRP neuron response to ghrelin, which in normal mice potently activates these neurons. Thus, both ghrelin-induced AgRP neuron activation (as determined by both Fos immunoreactivity and electrophysiology) and the associated hyperphagic response are blunted in mice consuming a HFD [47,48]. Yet the effect of ghrelin to induce calcium responses in AgRP neurons (measured by fiber photometry) remains largely intact in DIO animals at doses that fail to have any effect on feeding [14]. One potential explanation for this paradoxical outcome revolves around the fact that fiber photometry detects the changes of activity relative to a pre-intervention baseline but is not informative as to the number of neurons responding. Future studies using methods that allow recording individual populations of AgRP neurons (e.g., in vivo calcium imaging with mini-scopes and gradient refractive index (GRIN) lens implants) have the potential to determine if HFD feeding reduces the number of AgRP neurons activated in response to either ghrelin or a cold challenge.

Taken together, these data suggest that while HFD feeding does not block all AgRP neurons from responding to either ghrelin or cold exposure, it reduces the fraction of these neurons that responds to these stimuli and thus attenuates the associated hyperphagic response. Combined with evidence that HFD-feeding also blunts the feeding response to optogenetic AgRP neuron stimulation [14], suggesting that circuits lying downstream also become hyporesponsive, it is perhaps unsurprising that cold-induced hyperphagia is blocked.

In conclusion, we report that the normal coupling between thermoregulation and energy homeostasis is impaired by consuming a HFD. We further show that while AgRP neurons are activated by cold exposure in both chow- and HFD-fed mice, the number of AgRP neurons activated by cold appears to be reduced by HFD feeding, an effect associated with a failure to mount the expected hyperphagic response. Since cold-induced increases in energy expenditure remain intact in this setting, mice consuming a HFD are predisposed to weight loss during cold exposure in a manner not observed in mice consuming standard chow. A better understanding of the neurocircuitry linking thermoregulation to AgRP neuron activity, and how this system is impacted by HFD feeding, may ultimately inform the development of novel strategies for obesity treatment.

#### AUTHOR CONTRIBUTIONS

JDD, MWS and GJM conceived and designed the experimental approach. JDD, DT, CAW, KO, CLB, BNP, VD, MRB, JWS, GJM performed experiments and analyzed data. JDD, MWS and GJM prepared the manuscript. All authors edited the manuscript.

#### ACKNOWLEDGEMENTS

The authors gratefully acknowledge Dr. Richard Palmiter (University of Washington) for providing AgRP-Cre:GFP mice. The authors also thank

Kevin Velasco for assistance with biochemical measures and Jarrell Nelson for assistance with metabolic studies.

This work was supported by National Institutes of Health Grants DK089056 and DK124238 (to G.J.M.), DK083042 and DK101997 (to M.W.S.), K08 DK114474 and DK128383 (to J.M.S.), K01 DK126793 (to J.D.D.), R37DA033396 (to MRB), the NAPE Center Imaging and Circuits Core (P30 DA048736), the University of Washington Keck Imaging Center (S10-OD-016240), the Nutrition Obesity Research Center (DK035816), the Diabetes Research Center (DK17047), the Nutrition, Obesity, and Atherosclerosis (T32 HL007028; J.D.D.) and Diabetes, Obesity and Metabolism (T32 DK007247; C.A.W.) training grants at the University of Washington, a Department of Defense grant W81XWH2110635 (to J.M.S.), a Dick and Julia McAbee Endowed Fellowship (to J.D.D.), and an American Diabetes Association Innovative Basic Science Award (ADA 1-19-IBS-192, to G.J.M.) and Fellowship Grant (ADA 1-19-PDF-103, to J.D.D.)

#### DECLARATION OF COMPETING INTEREST

The authors declare that they have no known competing financial interests or personal relationships that could have appeared to influence the work reported in this paper.

#### DATA AVAILABILITY

Data will be made available on request.

#### APPENDIX A. SUPPLEMENTARY DATA

Supplementary data to this article can be found online at <https://doi.org/10.1016/j.molmet.2023.101835>.

#### REFERENCES

- [1] Deem JD, Faber CL, Pedersen C, Phan BA, Larsen SA, Ogimoto K, et al. Cold-induced hyperphagia requires AgRP neuron activation in mice. *Elife* 2020;9.
- [2] Gordon CJ. *Temperature regulation in laboratory rodents*. New York: Cambridge University Press; 1993.
- [3] Abreu-Vieira G, Xiao C, Gavrilova O, Reitman ML. Integration of body temperature into the analysis of energy expenditure in the mouse. *Mol Metabol* 2015;4(6):461–70.
- [4] Hahn TM, Breininger JF, Baskin DG, Schwartz MW. Coexpression of *Agrp* and *NPY* in fasting-activated hypothalamic neurons. *Nat Neurosci* 1998;1(4):271–2.
- [5] Schwartz MW, Woods SC, Porte Jr D, Seeley RJ, Baskin DG. Central nervous system control of food intake. *Nature* 2000;404(6778):661–71.
- [6] Krashes MJ, Koda S, Ye C, Rogan SC, Adams AC, Cusher DS, et al. Rapid, reversible activation of AgRP neurons drives feeding behavior in mice. *J Clin Invest* 2011;121(4):1424–8.
- [7] Aponte Y, Atasoy D, Sternson SM. AGRP neurons are sufficient to orchestrate feeding behavior rapidly and without training. *Nat Neurosci* 2011;14(3):351–5.
- [8] Atasoy D, Betley JN, Su HH, Sternson SM. Deconstruction of a neural circuit for hunger. *Nature* 2012;488(7410):172–7.
- [9] Betley JN, Xu S, Cao ZFH, Gong R, Magnus CJ, Yu Y, et al. Neurons for hunger and thirst transmit a negative-valence teaching signal. *Nature* 2015;521(7551):180–5.
- [10] Chen Y, Lin YC, Kuo TW, Knight ZA. Sensory detection of food rapidly modulates arcuate feeding circuits. *Cell* 2015;160(5):829–41.

- [11] Mandelblat-Cerf Y, Ramesh RN, Burgess CR, Patella P, Yang Z, Lowell BB, et al. Arcuate hypothalamic AgRP and putative POMC neurons show opposite changes in spiking across multiple timescales. *Elife* 2015;4.
- [12] Brown JM, Scarlett JM, Schwartz MW. Rethinking the role of the brain in glucose homeostasis and diabetes pathogenesis. *J Clin Invest* 2019;129(8):3035–7.
- [13] Deem JD, Faber CL, Morton GJ. AgRP neurons: regulators of feeding, energy expenditure, and behavior. *FEBS J* 2022;289(8):2362–81.
- [14] Beutler LR, Corpuz TV, Ahn JS, Kosar S, Song W, Chen Y, et al. Obesity causes selective and long-lasting desensitization of AgRP neurons to dietary fat. *Elife* 2020;9.
- [15] Mazzone CM, Liang-Guallpa J, Li C, Wolcott NS, Boone MH, Southern M, et al. High-fat food biases hypothalamic and mesolimbic expression of consummatory drives. *Nat Neurosci* 2020;23(10):1253–66.
- [16] Tong Q, Ye CP, Jones JE, Elmquist JK, Lowell BB. Synaptic release of GABA by AgRP neurons is required for normal regulation of energy balance. *Nat Neurosci* 2008;11(9):998–1000.
- [17] Franklin KBJ, Paxinos G. The mouse brain in stereotaxic coordinates. 4th ed. Academic Press; 2013.
- [18] Faber CL, Matsen ME, Meek TH, Krull JE, Morton GJ. Adaptable angled stereotaxic approach for versatile neuroscience techniques. *J Vis Exp* 2020;159.
- [19] Taicher GZ, Tinsley FC, Reiderman A, Heiman ML. Quantitative magnetic resonance (QMR) method for bone and whole-body-composition analysis. *Anal Bioanal Chem* 2003;377(6):990–1002.
- [20] Kaiyala KJ, Ogimoto K, Nelson JT, Muta K, Morton GJ. Physiological role for leptin in the control of thermal conductance. *Mol Metabol* 2016;5(10):892–902.
- [21] Kaiyala KJ, Ogimoto K, Nelson JT, Schwartz MW, Morton GJ. Leptin signaling is required for adaptive changes in food intake, but not energy expenditure, in response to different thermal conditions. *PLoS One* 2015;10(3):e0119391.
- [22] Weir JB. New methods for calculating metabolic rate with special reference to protein metabolism. *J Physiol* 1949;109(1–2):1–9.
- [23] Kaiyala KJ, Ogimoto K, Nelson JT, Muta K, Morton GJ. Physiological role for leptin in the control of thermal conductance. *Mol Metabol* 2016;5(10):892–902.
- [24] Tan CL, Cooke EK, Leib DE, Lin YC, Daly GE, Zimmerman CA, et al. Warm-sensitive neurons that control body temperature. *Cell* 2016;167(1):47–59. e15.
- [25] Faber CL, Matsen ME, Velasco KR, Damian V, Phan BA, Adam D, et al. Distinct neuronal projections from the hypothalamic ventromedial nucleus mediate glycemic and behavioral effects. *Diabetes* 2018;67(12):2518–29.
- [26] Fitzmaurice GM, Laird NM, Ware JH. Applied longitudinal analysis. John Wiley and Sons; 2012.
- [27] Trayhurn P, Thurlby PL, James WP. A defective response to cold in the obese (obob) mouse and the obese Zucker (fafa) rat [proceedings]. *Proc Nutr Soc* 1976;35(3):133A.
- [28] Trayhurn P, Thurlby PL, James WP. Thermogenic defect in pre-obese ob/ob mice. *Nature* 1977;266(5597):60–2.
- [29] Enriori PJ, Sinnayah P, Simonds SE, Garcia Rudaz C, Cowley MA. Leptin action in the dorsomedial hypothalamus increases sympathetic tone to brown adipose tissue in spite of systemic leptin resistance. *J Neurosci* 2011;31(34):12189–97.
- [30] Armitage G, Harris RB, Hervey GR, Tobin G. The relationship between energy expenditure and environmental temperature in congenitally obese and non-obese Zucker rats. *J Physiol* 1984;350:197–207.
- [31] Thurlby PL, Trayhurn P. The role of thermoregulatory thermogenesis in the development of obesity in genetically-obese (ob/ob) mice pair-fed with lean siblings. *Br J Nutr* 1979;42(3):377–85.
- [32] Brobeck JR. Food intake as a mechanism of temperature regulation. *Yale J Biol Med* 1948;20(6):545–52.
- [33] Yang S, Tan YL, Wu X, Wang J, Sun J, Liu A, et al. An mPOA-ARC(AgRP) pathway modulates cold-evoked eating behavior. *Cell Rep* 2021;36(6):109502.
- [34] Andrews ZB, Liu ZW, Wallingford N, Erion DM, Borok E, Friedman JM, et al. UCP2 mediates ghrelin's action on NPY/AgRP neurons by lowering free radicals. *Nature* 2008;454(7206):846–51.
- [35] Liu T, Kong D, Shah BP, Ye C, Koda S, Saunders A, et al. Fasting activation of AgRP neurons requires NMDA receptors and involves spinogenesis and increased excitatory tone. *Neuron* 2012;73(3):511–22.
- [36] Smith CK, Romsos DR. Cold acclimation of obese (ob/ob) mice: effects of energy balance. *Metabolism* 1984;33(9):853–7.
- [37] Hamilton CL. Interactions of food intake and temperature regulation in the rat. *J Comp Physiol Psychol* 1963;56:476–88.
- [38] Johnson RE, Kark RM. Environment and food intake in man. *Science* 1947;105(2728):378–9.
- [39] Cannon B, Nedergaard J. Thermogenesis challenges the adipostat hypothesis for body-weight control. *Proc Nutr Soc* 2009;68(4):401–7.
- [40] Cui X, Nguyen NL, Zarebidaki E, Cao Q, Li F, Zha L, et al. Thermoneutrality decreases thermogenic program and promotes adiposity in high-fat diet-fed mice. *Physiol Rep* 2016;4(10).
- [41] Hoevenaars FP, Bekkenkamp-Groenestein M, Janssen RJ, Heil SG, Bunschoten A, Hoek-van den Hil EF, et al. Thermoneutrality results in prominent diet-induced body weight differences in C57BL/6J mice, not paralleled by diet-induced metabolic differences. *Mol Nutr Food Res* 2014;58(4):799–807.
- [42] Rippe C, Berger K, Boiers C, Ricquier D, Erlanson-Albertsson C. Effect of high-fat diet, surrounding temperature, and enterostatin on uncoupling protein gene expression. *Am J Physiol Endocrinol Metab* 2000;279(2):E293–300.
- [43] Small L, Gong H, Yassmin C, Cooney GJ, Brandon AE. Thermoneutral housing does not influence fat mass or glucose homeostasis in C57BL/6 mice. *J Endocrinol* 2018;239(3):313–24.
- [44] Valdes S, Maldonado-Araque C, Garcia-Torres F, Goday A, Bosch-Comas A, Bordiu E, et al. Ambient temperature and prevalence of obesity in the Spanish population: the Di@bet.es study. *Obesity (Silver Spring)* 2014;22(11):2328–32.
- [45] Yang HK, Han K, Cho JH, Yoon KH, Cha BY, Lee SH. Ambient temperature and prevalence of obesity: a nationwide population-based study in Korea. *PLoS One* 2015;10(11):e0141724.
- [46] Betley JN, Cao ZF, Ritola KD, Sternson SM. Parallel, redundant circuit organization for homeostatic control of feeding behavior. *Cell* 2013;155(6):1337–50.
- [47] Briggs DI, Enriori PJ, Lemus MB, Cowley MA, Andrews ZB. Diet-induced obesity causes ghrelin resistance in arcuate NPY/AgRP neurons. *Endocrinology* 2010;151(10):4745–55.
- [48] Briggs DI, Lockie SH, Benzler J, Wu Q, Stark R, Reichenbach A, et al. Evidence that diet-induced hyperleptinemia, but not hypothalamic gliosis, causes ghrelin resistance in NPY/AgRP neurons of male mice. *Endocrinology* 2014;155(7):2411–22.